Learning Micro-Macro Models for Traffic Control Using Microscopic Data

Jonathan Krook, Mladen Čičić, Karl Henrik Johansson

Learning Micro-Macro Models for Traffic Control Using Microscopic Data

Jonathan Krook Mladen Čičić Karl Henrik Johansson

***Abstract*—Connected and Automated Vehicles (CAVs) are likely to have a large impact on the traffic in the near future. Assuming we are able to communicate some commands directly to them, it is of interest to know how CAVs can be used for traffic control. In order to achieve this, we need to understand how such controls affect the rest of the traffic. In this work, we study the influence of a CAV acting as a moving bottleneck, using the CAV's speed as a control input. We discuss the interpretation of the microscopic traffic data in the macroscopic framework, and propose nonparametric methods for learning the micro-macro model describing the interaction between the CAV and the surrounding traffic. We use only the local traffic data in the vicinity of the CAV, and design simple, targeted data collection experiments. This learned model is then used to predict the evolution of the traffic, and the predictions are compared with corresponding data from microscopic simulations.**

I. Introduction

One of the most lauded potential benefits of Connected and Automated Vehicles (CAVs) is their contribution to increased road throughput [1], increasing safety and flow stability, despite their generally more conservative driving behaviour compared to human drivers [2]. Unless eclipsed by network-wide phenomena, e.g. induced demand, this improvement should reduce congestion, and emissions. Additionally, a new traffic control paradigm is becoming viable, using CAVs within the traffic as sensors and actuators, collecting local traffic measurements, and issuing reference speeds or other commands to them as control inputs. Thus, in order to implement such control laws, the effects of these control inputs need to be well understood and properly modeled.

Both the microscopic and the macroscopic traffic modelling paradigm have own advantages and disadvantages regarding capturing the influence of individual vehicles on the rest of the traffic. In microscopic models, the behaviour of each vehicle is described separately, allowing for easy implementation of CAV-actuated traffic control. While their implementation in microscopic traffic simulators such as SUMO [3] is widely accepted to be a good representation of the actual traffic, these models are, prohibitively computationally expensive and hard to use as prediction models for calculating the control inputs. On the other hand, macroscopic models such as the Lighthill-Whitham-Richards (LWR) model [4] describe the aggregate behaviour of the traffic, and are thus applicable for analysing and predicting the evolution of the traffic state.

Micro-macro approaches combining these two paradigms have recently been garnering much attention, as the aggregate behaviour of vehicles in microscopic models has been shown to converge to its macroscopic counterpart [5, 6]. Macroscopic quantities may be obtained from the microscopic data by using e.g. kernel estimation [7]. One of the most direct ways a CAV can influence the rest of the traffic is by reducing its speed and acting as a moving bottleneck [8, 9], which has been considered for traffic control [10, 11, 12]. Before this type of traffic control can be implemented, more work is required on identifying and validating the model of this interaction using real and synthetic traffic data.

The problem of fitting the flux function of the traffic (i.e., the fundamental diagram) to measurements has been approached from many perspectives [13, 14]. Conventionally, a parametric form of the flux function is assumed, and then calibrated using the collected traffic measurements. Similarly, the moving bottleneck flux function can be estimated using the measurements of the overtaking flow [15].

In this paper, we study the influence of a controlled vehicle acting as a moving bottleneck on the surrounding traffic, using microscopic traffic simulation data. We model the interaction between them by assuming the traffic at the position of the moving bottleneck is governed by a different flux function, using the LWR model with space-dependent flux functions. By assuming both of these flux functions are continuous and piecewise-linear, we are able to fit them nonparametrically, and can use the Front-tracking Transition System Model (FTSM) [16] to predict the evolution of traffic. We design experiments including a single controlled vehicle, and obtain local measurements of the traffic state in its vicinity. This data is used to simultaneously learn the flux functions of the moving bottleneck and the rest of the traffic. Finally, the predictions acquired from the learned model are compared against the simulation data.

The remainder of the paper is organized as follows. In Section II, we discuss a macroscopic model for traffic flow with a moving bottleneck, describe how it is connected to the microscopic traffic data, and outline the traffic prediction model learning problem. Next, in Section III, we propose the structure of the prediction model, describe the data collection experiments, and present methods for learning the flux functions used in the model from microscopic data. Thereafter, in Section IV, we present a numerical evaluation of the proposed traffic prediction model learning methods through simulations, and finally conclude in Section V.

J. Krook and K.H. Johansson (jkroo@kth.se, kallej@kth.se) are with the Division of Decision and Control System, KTH Royal Institute of Technology, Sweden. M. Čičić (mladen.cicic@gipsa-lab.fr) is with Univ. Grenoble Alpes, CNRS, Inria, Grenoble INP, GIPSA-lab, France.

This work has received funding from the KAUST Office of Sponsored Research under Award No. OSR-2019-CRG8-4033, VINNOVA within the FFI program under contract 2014-06200, the Swedish Research Council, the Swedish Foundation for Strategic Research, Knut and Alice Wallenberg Foundation, and the European Research Council (ERC) under the European Union's Horizon 2020 research and innovation programme (grant agreement 694209), http://scalefreeback.eu

II. Preliminaries and problem formulation

In this section we give some preliminaries, defining the macroscopic traffic model that will be used and the connections between its states and microscopic traffic data. Then, we outline the traffic prediction model learning problem which will be tackled in the following section.

A. Macroscopic traffic model

The evolution of the traffic state on the considered road segment can be described by the Lighthill-Whitham Richards model [4] with space-dependent flux function, given by

$$\partial_t \rho(x,t) + \partial_x Q(\rho(x,t),x,t) = 0, \tag{1}$$

where we denote by x the position along the road, t the time, $\rho(x,t)$ the traffic density at position x and time t, and $Q(\rho,x,t)$ the flux function. We let the flux function $Q(\rho,x,t)$ be piecewise defined in space and time, with different flux functions $Q_i(\rho)$ mapping the traffic density to the traffic flow in each interval $x \in (X_{i-1}(t), X_i(t))$.

In particular, we model the influence of a controlled vehicle ξ slowing down to some constant low speed u_ξ and acting as a moving bottleneck, restricting the capacity of the road around it, by using a space-dependent flux function

$$Q(\rho,x,t) = \begin{cases} Q_0(\rho), & x < x_\xi(0) - l_\xi + u_\xi t, \\ Q_\xi(\rho), & x_\xi(0) - l_\xi + u_\xi t < x < x_\xi(0) + u_\xi t, \\ Q_0(\rho), & x_\xi(0) + u_\xi t < x, \end{cases} \tag{2}$$

for $t \in [t^\xi_{\text{slow}}, t^\xi_{\text{fast}}]$ when we assume the controlled vehicle travels at constant speed $\dot{x}_\xi(t) = u_\xi$. Here, we denote by $x_\xi(t) = x_\xi(0) + u_\xi t$ the position of the front of the controlled vehicle, l_ξ its length, Q_0 the flux function of the unimpeded road, with homogeneous geometry, and Q_ξ the reduced flux function for the portion of the road where one of the lanes is blocked by the moving bottleneck.

Letting $l_\xi \to 0$, in order for the Rankine-Hugoniot condition to hold on the up- and downstream boundary of the zone described by flux function Q_ξ, we require that

$$\begin{aligned} Q_\xi(\rho_\xi) - Q_0(\rho_-) &= u_\xi(\rho_\xi - \rho_-), \\ Q_0(\rho_+) - Q_\xi(\rho_\xi) &= u_\xi(\rho_+ - \rho_\xi), \end{aligned}$$

where $\rho_- = \rho((x_\xi(t))_-, t)$ and $\rho_+ = \rho((x_\xi(t))_+, t)$ are the traffic densities immediately upstream and downstream of the controlled vehicle, respectively, and ρ_ξ is the traffic density in the zone described by Q_ξ. The traffic flow overtaking the controlled vehicle is given by

$$\omega_\xi(t) = \min\left\{ Q_0(\rho_-) - u_\xi \rho_-, \max_{\rho \geq 0} \left(Q_\xi(\rho) - u_\xi \rho \right) \right\}.$$

Assuming both Q_0 and Q_ξ can be approximated as continuous piecewise-linear functions, the solution to (1), with piecewise-constant initial conditions

$$\rho(x,0) = \begin{cases} \rho_1, & x < X_1, \\ \quad \vdots & \\ \rho_i, & X_{i-1} < x < X_i, \\ \quad \vdots & \\ \rho_{N+1}, & X_N < x, \end{cases}$$

and $Q(\rho,x,t)$ given by (2) can be found exactly using the front-tracking method [17]. This approach was formalised as a transition system in [16], and the FTSM given therein will be used to predict the evolution of the system state. Additionally, assuming this form of flux functions allows us to employ nonparametric methods to fit them.

B. Connection with microscopic traffic data

The traffic state of microscopic traffic models is given by describing the dynamics of each vehicle. For each vehicle $i \in \mathcal{I}(t)$, where $\mathcal{I}(t)$ is the set of indices of all vehicle on the road at time t, its trajectory $x_i(t)$ is determined by

$$\begin{aligned} \dot{x}_i(t) &= v_i(t), \\ \dot{v}_i(t) &= a_i(t), \end{aligned}$$

where its acceleration $a_i(t)$ depends on the state of nearby vehicles, and is determined by some car-following (e.g. Intelligent Driver Model (IDM) [18]), and lane-changing model.

Considering a road segment $x \in [X_\text{l}, X_\text{r}]$, we may calculate the macroscopic average traffic density and harmonic mean traffic speed of the vehicles in it. Denoting by $\mathcal{I}^{X_\text{r}}_{X_\text{l}}(t) \subset \mathcal{I}(t)$ the set of indices of all vehicles on $[X_\text{l}, X_\text{r}]$,

$$\mathcal{I}^{X_\text{r}}_{X_\text{l}}(t) = \{ i \in \mathcal{I}(t) : X_\text{l} \leq x_i(t) \leq X_\text{r} \},$$

we can write the mean traffic density of the segment as

$$\bar{\rho}^\delta(X_\text{l}, X_\text{r}, t) = \frac{\left| \mathcal{I}^{X_\text{r}}_{X_\text{l}}(t) \right|}{X_\text{r} - X_\text{l}} = \frac{\int_{X_\text{l}}^{X_\text{r}} \sum_{i \in \mathcal{I}(t)} \delta(x - x_i(t)) \mathrm{d}x}{X_\text{r} - X_\text{l}},$$

where $|\cdot|$ denotes set cardinality, and δ is the Dirac delta function. Similarly, the harmonic mean speed is given by

$$\bar{v}^\delta(X_\text{l}, X_\text{r}, t) = \frac{\left| \mathcal{I}^{X_\text{r}}_{X_\text{l}}(t) \right|}{\sum_{i \in \mathcal{I}^{X_\text{r}}_{X_\text{l}}(t)} \frac{1}{v_i(t)}} = \frac{\int_{X_\text{l}}^{X_\text{r}} \sum_{i \in \mathcal{I}(t)} \delta(x - x_i(t)) \mathrm{d}x}{\int_{X_\text{l}}^{X_\text{r}} \sum_{i \in \mathcal{I}(t)} \frac{\delta(x - x_i(t))}{v_i(t)} \mathrm{d}x}.$$

In order to capture the effect individual vehicles have on their vicinity, as well as to smooth the traffic density, we represent the presence of a vehicle with a Gaussian kernel centered on its position instead of a Dirac delta. This allows us to define the traffic density at any point of the road as

$$\check{\rho}(x,t) = \sum_{i \in \mathcal{I}(t)} \frac{1}{L} \varphi\left(\frac{x - x_i(t)}{L} \right), \tag{3}$$

where φ is the unit Gaussian kernel, and L is an empirical parameter reflecting the range in which individual vehicles directly influence the behaviour of vehicles around them. The traffic speed and flow at any point on the road are then

$$\begin{aligned} \check{v}(x,t) &= \frac{\check{\rho}(x,t)}{\sum_{i \in \mathcal{I}(t)} \frac{\varphi\left(\frac{x - x_i(t)}{L} \right)}{L v_i(t)}}, \\ \check{q}(x,t) &= \check{\rho}(x,t) \check{v}(x,t). \end{aligned} \tag{4}$$

The flow of vehicles overtaking the controlled vehicle ξ can be calculated by counting the overtaking vehicles within some time interval $t \in [t_1, t_2]$,

$$\bar{\omega}^\delta_\xi(t_1, t_2) = \frac{\left| \mathcal{I}^\infty_{x_\xi(t_2)}(t_2) \right| - \left| \mathcal{I}^\infty_{x_\xi(t_1)}(t_1) \right|}{t_2 - t_1},$$

which yields Gaussian kernel instantaneous overtaking flow

$$\check{\omega}_\xi(t) = \sum_{i \in \mathcal{I}(t)} \frac{v_i(t) - v_\xi(t)}{L} \varphi\left(\frac{x_i(t) - x_\xi(t)}{L} \right).$$

C. Problem formulation

In practice, the traffic model is not likely to be known a priori, and would instead need to be identified from experimental data. We study the problem of learning a prediction model for the evolution of the traffic state on a road segment, that captures the influence of a slow-moving CAV on the rest of the traffic. Describing the evolution of traffic by (1) and (2), the problem reduces to finding flux functions Q_0 and Q_ξ, assumed to be continuous and piecewise-linear.

We assume that the only traffic data available are the trajectories of vehicles close to CAV ξ, and that we can collect these measurements from multiple experiments, selecting different CAV control inputs for each experiment. The traffic state prediction is intended to be used to calculate the control actions, typically by predicting the future flow through some point on the road, given the control action at the current time. Therefore, for each experiment s, we use the relative difference in the total flow through some point X_q downstream of the controlled vehicle, from some start time t_q^0 until time $t_q^{\xi,s}$ when the controlled vehicle ξ reaches X_q, $x_\xi^s(t_q^{\xi,s}) = X_q$,

$$e^s = 1 - \left(\int_{t_q^0}^{t_q^{\xi,s}} \hat{q}(X_q,t)\mathrm{d}t \right) \left(\int_{t_q^0}^{t_q^{\xi,s}} \check{q}(X_q,t)\mathrm{d}t \right)^{-1} \tag{5}$$

to evaluate prediction accuracy and model performance.

III. Traffic prediction model learning

We now propose a solution to the traffic model learning problem. First, we outline the overall procedure of building a traffic prediction model and using it to predict the flow downstream of the controlled CAV. Then, methods for learning the model components are described.

A. Solution structure

The evolution of traffic state given the control actions of a CAV acting as a moving bottleneck can be predicted using the FTSM [16], given that continuous piecewise-linear flux functions Q_0 and Q_ξ are known. In order to gather the relevant measurements, we design experiments $s \in \mathcal{S}$, where the controlled vehicle ξ slows down to speed u_ξ^s at some time t_{slow}^ξ, and speeds up again at time t_{fast}^ξ. During $t \in [t_{\text{slow}}^\xi, t_{\text{fast}}^\xi]$, we collect local traffic state measurement directly upstream and downstream of the controlled vehicle ξ, given by (ρ_-^s, q_-^s) and (ρ_+^s, q_+^s), respectively, as well as measure the overtaking flow ω_ξ^s. We assume that the traffic flows can be measured indirectly, by measuring the space-averaged traffic speed $v_\pm^s$, $q_\pm^s = \rho_\pm^s v_\pm^s$. Experiments are executed for different reference speeds u_ξ^s and levels of inflow at the start of the road segment q_{in}^s, $s \in \mathcal{S}$.

Once Q_0 and Q_ξ are learned, we may use the resulting prediction model to predict the traffic density evolution $\hat{\rho}(x,t)$. For each experiment, the prediction is calculated at time $t = 0$, before CAV ξ enters the road, assuming only the average traffic inflow to the considered road segment q_{in}^s is known. Mimicking the simulation scenario, the traffic density of the prediction model is initialized at $t = 0$ to

$$\hat{\rho}(x,0) = \begin{cases} Q_0^{-1}(q_{\text{in}}^s), & x < 0, \\ 0, & x > 0, \end{cases}$$

where $x = 0$ is the position of the start of the road segment. Until the time t_0^ξ, when the controlled vehicle arrives, the traffic flow on the whole road is modeled by Q_0. At time t_0^ξ, a zero-length zone described by flux function Q_ξ, with its boundaries moving at the reference speed of the controlled vehicle $\lambda_\xi^\pm = v_\xi^{\max}$, is added to the prediction model. The propagation speed of these boundaries is reduced to $\lambda_\xi^\pm = u_\xi^s$ at time t_{slow}^ξ, potentially causing congestion to start accumulating, and then returned to $\lambda_\xi^\pm = v_\xi^{\max}$ at t_{fast}^ξ. Finally, the predicted flow through a downstream point X_q in (5) is

$$\hat{q}(X_q,t) = Q_0\left(\hat{\rho}(X_q,t)\right).$$

B. Learning the traffic flux function Q_0

According to (1), (2), if CAV ξ is travelling at a speed u_ξ slower than the surrounding traffic, it will act as a moving bottleneck, and, given a high enough traffic inflow q_{in}, cause a traffic density discontinuity at its position,

$$\rho(x,t) = \begin{cases} \rho_-, & x < x_\xi(t), \\ \rho_+, & x > x_\xi(t), \end{cases}$$

for $x \approx x_\xi(t)$. Here, ρ_- and ρ_+ both need to satisfy

$$\omega_\xi = Q_0(\rho) - u_\xi \rho,$$

where ω_ξ is the flow overtaking the CAV ξ, and all collected measurements should follow $Q_0(\rho_\pm^s) = q_\pm^s$.

We assume that the traffic flux function Q_0 is concave, with $Q_0(0) = Q_0(P) = 0$, where P is the jam density which can be set empirically as the bumper-to-bumper traffic density. Then Q_0 can be approximated as an upper concave envelope of points $\mathcal{M}$,

$$Q_0(\rho) = \inf\{\mathcal{Q}(\rho) | (\forall (\rho,q) \in \mathcal{M}) \mathcal{Q}(\rho) \geq q, \mathcal{Q} \text{ concave on } [0,P]\},$$

$$\mathcal{M} = \{(0,0),(P,0)\} \cup \{(\rho_-^s, q_-^s) | s \in \mathcal{S}\} \cup \{(\rho_+^s, q_+^s) | s \in \mathcal{S}\},$$

and as such is a continuous piecewise-linear function. By executing experiments with a wide range of different moving bottleneck speeds u_ξ^s, $s \in \mathcal{S}$, we are able to sample different points on Q_0, covering the most relevant part of the flux function. As the set of experiments grows, we may approximate any continuous concave flux function with thus defined Q_0 arbitrarily well.

The described fitting method tacitly assumes that the measured traffic state follows the flux function Q_0 exactly. In presence of noise and variability of human driving behaviour, the method produces an overestimation of the flux function. Therefore, it is important that the influence of noise is eliminated as much as possible from measurements $(\rho_\pm^s, q_\pm^s)$, $s \in \mathcal{S}$, e.g. by averaging the measurements over a long time horizon and only considering the steady-state measurements.

C. Learning the moving bottleneck flux function Q_ξ

Using the measurements from the same set of experiments, we can identify the moving bottleneck flux function Q_ξ simultaneously with identifying the traffic flux function Q_0. Although points of this function cannot be directly measured, we may use the fact that lines $\omega_\xi^s + u_\xi^s \rho$, $s \in \mathcal{S}$ should be tangent to Q_ξ to learn the relevant parts of Q_ξ, allowing us to capture the influence of moving bottlenecks. We have

$$Q_\xi(\rho) \leq \omega_\xi^s + u_\xi^s \rho, \quad \rho \in [0, P_\xi] \tag{6}$$

where $P_\xi \approx \beta P$ is the jam density of the moving bottleneck flux functions, and β is the ratio of lanes not occupied by the moving bottleneck to the total number of lanes.

Thus, we can upper-bound $Q_\xi(\rho) \le \hat{Q}_\xi(\rho)$ by

$$\hat{Q}_\xi(\rho) = \sup\{\mathcal{Q}(\rho) | \mathcal{Q}(\rho) \le \omega_\xi^s + u_\xi^s \rho, \rho \in [0, P_\xi], s \in \mathcal{S}\},$$

according to (6), with $Q_\xi(\rho) = \hat{Q}_\xi(\rho)$ for those ρ in which lines $\omega_\xi^s + u_\xi^s \rho$, $s \in \mathcal{S}$ are tangent to Q_ξ. As long as Q_ξ follows the aforementioned constraints, its exact shape is inconsequential, so we approximate it by a continuous piecewise-linear function concave on $[0, P_\xi]$,

$$Q_\xi(\rho) = \sup\left\{ v_{\max}\rho, \hat{Q}_\xi(\rho), \frac{\hat{Q}_\xi(\beta\sigma_0^{\max})(P_\xi - \rho)}{P_\xi - \beta\sigma_0^{\max}} \right\},$$
$$\sigma_0^{\max} = \arg\max_{\rho \in [0,P]} Q_0(\rho).$$

We select this form for $Q_\xi(\rho)$, $\rho \in [\beta\sigma_0^{\max}, P_\xi]$ in order to make Q_ξ achieve maximum for $\rho = \beta\sigma_0^{\max}$.

The influence of noise and behavioural variability is even more pronounced in case of fitting Q_ξ than for Q_0, and the described method produces an underestimation of Q_ξ. In this case, it can be beneficial to use a parametric approach, assuming a triangular from of Q_ξ,

$$Q_\xi^\Delta(\rho) = q_\xi^{\max} \min\left\{ \frac{\rho}{\sigma_\xi^{\max}}, \frac{P_\xi - \rho}{P_\xi - \sigma_\xi^{\max}} \right\},$$

which is parametrized by the critical density $\sigma_\xi^{\max}$, capacity $q_\xi^{\max}$, and jam density $P_\xi \approx \beta P$. The point $(\sigma_\xi^{\max}, q_\xi^{\max})$ can be calculated as a least-squares fit,

$$(\sigma_\xi^{\max}, q_\xi^{\max}) = \arg\min_{(\rho,q)\in([0,P],\mathbb{R}_{\ge 0})} \sum_{s\in\mathcal{S}} \left(\omega_\xi^s + u_\xi^s \rho - q\right)^2.$$

IV. Numerical evaluations

A. Simulation set-up

We executed the simulations in SUMO [3], using the Intelligent Driver Model as the car-following model and the default lane-changing model. Model parameters were based on those given in [2], selected to reflect realistic driver behaviour, and can be found in Table I. We conducted preliminary simulations in order to determine the parameters that produce reasonable lane-changing behaviour, and found that lcAssertive= 3 achieves good results.

The simulations take place on a 30 km long two-lane road segment. We execute $K = 5$ simulation runs for each simulation scenario $s \in \mathcal{S}$ defined by the inflow to the road q_{in}^s, and control vehicle reference speed u_ξ^s. The traffic enters the road at $t = 0$, at inflow level q_{in}^s, and the controlled vehicle is introduced to the road at $t_0^\xi = 100$ s, with default reference speed set to $v_\xi^{\max} = 100$ km/h. Then, at $t_{\text{slow}}^\xi = 250$ s, we reduce the reference speed of the controlled vehicle to u_ξ^s, and at $t_{\text{fast}}^\xi = 750$ s increase it back to $v_\xi^{\max} = 100$ km/h. The simulation ends at $t_{\text{end}} = 1000$ s.

accel	2.6 m/s^2	maxSpeed	30 m/s
decel	7.4 m/s^2	lcSpeedGain	0.887
length	5 m	lcKeepRight	0.835
minGap	2.5 m	lcAssertive	3

TABLE I: Parameters used for microscopic simulations.

All measurements from the simulations were collected with sampling period of $T = 10$ s using TraCI, and then preprocessed in a Python script to obtain suitable data for fitting flux functions Q_0 and Q_ξ, and provide illustrations and comparison with the predicted data. The main data processing was done in MATLAB. Only the local measurements in the vicinity of the controlled vehicle ξ are used for flux function fitting. Traffic densities $\check{\rho}(x,t)$ and flows $\check{q}(x,t)$ are calculated from the trajectories of the simulated vehicles according to (3) and (4), with influence range $L = 50$ m. For the overtaking flow measurements, we simply count the number of vehicles that overtake the controlled vehicle within the sampling period T, and use $\bar{\omega}_\xi^\delta(t-T,t)$.

When calculating points $(\rho_\pm^s, q_\pm^s)$ for fitting Q_0, we used a single value for each scenario s. In order to reduce the influence of noise and eliminate transient behaviour, we calculate these values by using the averaged "steady state" measurements. For each measurement f (either ρ or q), scenario s, and simulation run k, the "steady state" interval $[t_{\text{ss}}^{\xi,\bar{f}_\pm^{s,k}}, t_{\text{fast}}^\xi]$,

$$t_{\text{ss}}^{\xi,\bar{f}_\pm^{s,k}} = \min\left\{ t \in [t_{\text{slow}}^\xi, t_{\text{fast}}^\xi] \,\middle|\, \left(\forall\tau \in [t, t_{\text{fast}}^\xi]\right) \left| 1 - \frac{\bar{f}_\pm^{s,k}(\tau)}{\bar{f}_\pm^{s,k}(t_{\text{fast}}^\xi)} \right| \le C \right\},$$

when the relative deviation of the measurement from its value at time t_{fast}^ξ is not larger than some constant C. Here, $\bar{f}_-(t)$ and $\bar{f}_+(t)$ are the measurements upstream and downstream of the controlled vehicle ξ, respectively,

$$\bar{f}_-^{s,k}(t) = \bar{f}^{s,k}(x_\xi^{s,k}(t) - 2L, x_\xi^{s,k}(t), t).$$
$$\bar{f}_+^{s,k} = \bar{f}^{s,k}(x_\xi^{s,k}(t) + L, x_\xi^{s,k}(t) + 3L, t).$$

Finally, we calculate $(\rho_\pm^s, q_\pm^s)$ as

$$f_\pm^s = \left(K\left(t_{\text{fast}}^\xi - t_{\text{ss}}^{\xi,\bar{f}_\pm^{s,k}}\right)\right)^{-1} \sum_{k=1}^{K} \int_{t_{\text{ss}}^{\xi,\bar{f}_\pm^{s,k}}}^{t_{\text{fast}}^\xi} \bar{f}_\pm^{s,k}(t)\mathrm{d}t. \quad (7)$$

B. Simulation results

Finally, we put the presented flux function learning methods, and the FTSM prediction model, to test, by executing the second batch of simulations, with $(q_{\text{in}}^s, u_\xi^s) \in q_{\text{in}}^{\mathcal{S}_{Q,1}} \times u_\xi^{\mathcal{S}_{Q,1}} \cup q_{\text{in}}^{\mathcal{S}_{Q,2}} \times u_\xi^{\mathcal{S}_{Q,2}}$. The first set, $q_{\text{in}}^{\mathcal{S}_{Q,1}} \times u_\xi^{\mathcal{S}_{Q,1}}$,

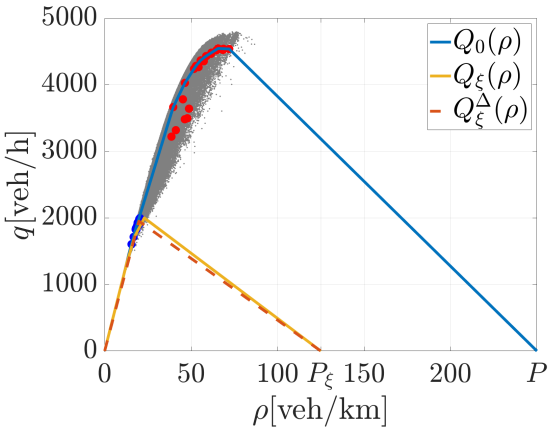

Fig. 1: Flux functions Q_0, Q_ξ, and Q_ξ^Δ (parametrically estimated), learned from simulation data.

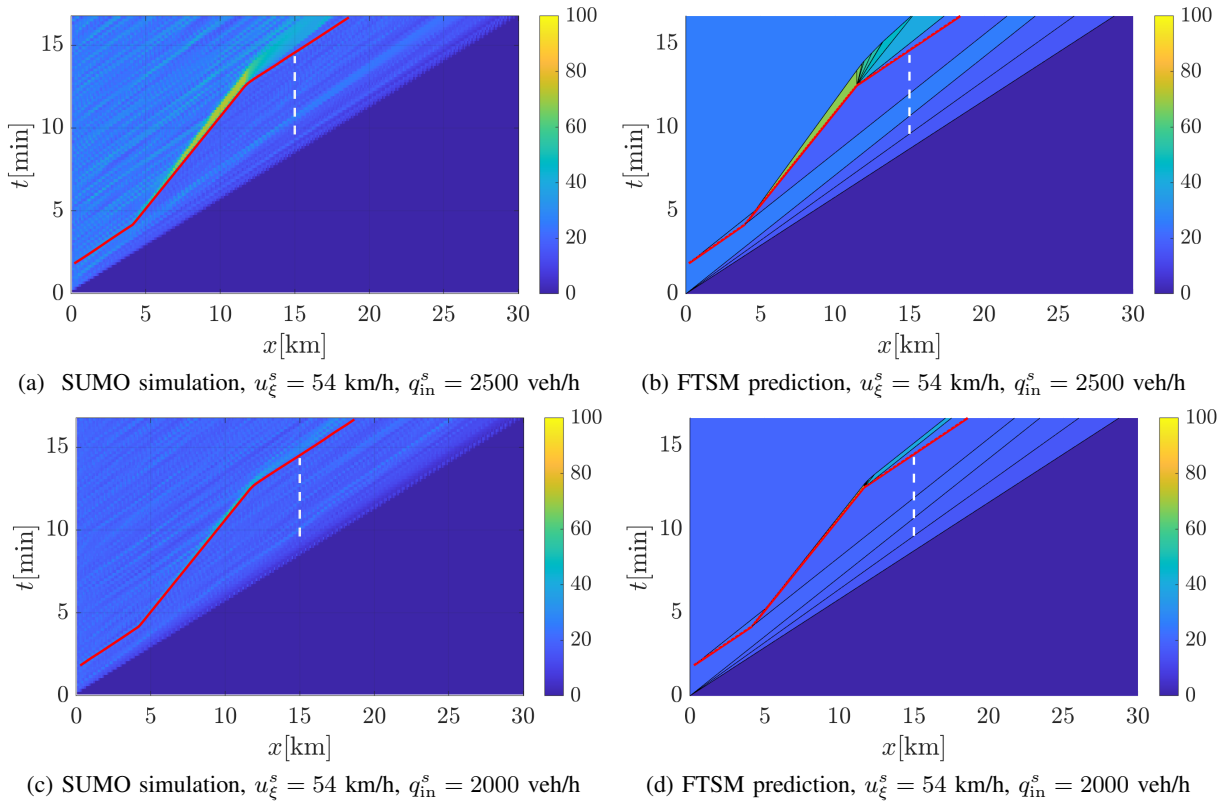

(a) SUMO simulation, $u_\xi^s = 54$ km/h, $q_{\text{in}}^s = 2500$ veh/h

(b) FTSM prediction, $u_\xi^s = 54$ km/h, $q_{\text{in}}^s = 2500$ veh/h

(c) SUMO simulation, $u_\xi^s = 54$ km/h, $q_{\text{in}}^s = 2000$ veh/h

(d) FTSM prediction, $u_\xi^s = 54$ km/h, $q_{\text{in}}^s = 2000$ veh/h

Fig. 2: Comparison between the traffic density of the SUMO simulations and FTSM predictions for two scenarios. Traffic density is colour-coded, with warmer colours signifying denser traffic.

gives us a dense sampling of regular operating conditions, with $q_{\text{in}}^{\mathcal{S}_{Q1}} = \{2000, 2200, 2400\}$ veh/h, and reference speeds $u_\xi^{\mathcal{S}_{Q1}} = \{54, 57.6, 61.2, 64.8, 68.4, 72\}$ km/h, and the second set considers a wider range of u_ξ^s in case of high inflow, with $q_{\text{in}}^{\mathcal{S}_{Q2}} = \{2500\}$ veh/h, and $u_\xi^{\mathcal{S}_{Q2}} = \{50.4, 57.6, 64.8, 72, 79.2, 86.4\}$ km/h.

The nonparametrically learned flux functions Q_0 and Q_ξ, as well as the parametrically learned Q_ξ^Δ, are shown in Fig. 1. The measurement collected everywhere on the considered road are shown by grey points, and averaged downstream and upstream measurements $(\rho_\pm^s, q_\pm^s)$, defined by (7), are shown by blue and red points, respectively. The two methods of learning Q_ξ yield similar results, both achieving a maximum of approximately 2000 veh/h, consistent with the observations of the previous simulations batch.

The conspicuous absence of data points in the congestion regime, for $\rho > 70$ veh/km, is a result of lack of simulation runs with very low moving bottleneck speeds, omitted because such reference speeds are likely to be outside of the permitted control input range, and could be hazardous. If scenarios with any $u_\xi \geq 0$ are allowed, we are able to estimate Q_0 for densities up to maximum ρ for which $Q_0(\rho) \geq q_\xi^{\max}$. Note that for very low u_ξ, the overtaking flow is not well represented by a single moving bottleneck flux function Q_ξ, and we need to instead consider Q_ξ dependent on u_ξ.

In Fig. 2 we show a comparison of the evolution of the simulated and predicted traffic density in two scenarios. We use the parametrically learned Q_ξ^Δ as the moving bottleneck flux function in the FTSM-based prediction model. Fig. 2a and 2c show the Gaussian-smoothed aggregate traffic density (3), based on vehicle trajectories from SUMO simulations with $q_{\text{in}} = 2500$ veh/h and $q_{\text{in}} = 2000$ veh/h respectively, and Fig. 2b and 2d show the FTSM-based prediction for the corresponding scenarios. We can see that in case of high incoming traffic flow $q_{\text{in}} = 2500$ veh/h, the FTSM-based prediction captures the buildup of congestion after the controlled vehicle slows down, as well as its discharge after the controlled vehicle speeds up again. Interestingly, the predicted time when the congestion is discharged is very close to the one observed in SUMO simulation, even though only the local measurements in the vicinity of the moving bottleneck while it was active were used for model learning. For $q_{\text{in}} = 2000$ veh/h, we correctly predict that almost no congestion builds up in the wake of the controlled vehicle.

A more quantitative way to compare the predictions to simulations is by considering the relative difference in the total flow through some point defined by (5). We measure the cumulative flow through point $X_q = 15$ km during the time interval indicated in Fig. 2 by dashed white lines, from $t_q^0 = 9.6$ min until the time the controlled vehicle reaches X_q. This relative prediction error over the five executed simulation runs for each scenarios shown in Fig. 3. We can see that the average e^s is consistently negative for all scenarios, so an alternative way to calibrate the moving bottleneck flux function could be by minimising the absolute average of this performance index.

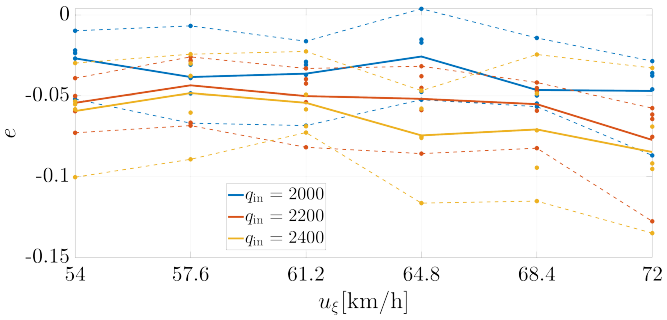

Fig. 3: Relative prediction error of the cumulative flow through $X_q = 15$ km. Solid lines are average errors and dashed lines are minimum and maximum errors.

V. Conclusions

In this work, we discuss using local traffic measurements in the vicinity of a controlled vehicle to learn a model of how it affects the rest of the traffic. The traffic measurements were acquired from the microscopic traffic data from simulations executed in SUMO, on a two-lane highway. We showed that a slow-moving controlled vehicle can be modelled as a moving bottleneck, through describing the traffic flow with a different flux function at the controlled vehicle's position. The same experimental set-up was used to simultaneously learn the flux function of the moving bottleneck and the flux function of the rest of the traffic. Thus learned flux functions were used in FTSM to predict the traffic state evolution, which was shown to be close to the simulation results. The prediction model captured all the relevant interaction mechanisms, with the predicted cumulative overtaking flow within 10% of its simulated counterpart on average.

While the work presented herein relies on simulations, the methodology is fully able to incorporate real-world measurements. As a requirement for autonomous driving, CAVs need to track the trajectories of all vehicles in their vicinity using on-board sensors, and this data could readily replace the synthetic data acquired in simulations. Additionally, more general scenarios should be considered, with multiple connected vehicles, more complex manoeuvres, and different road geometries. Finally, the learned prediction model is intended to be used in traffic control implementation, using controlled moving bottlenecks for congestion dissipation in microscopic simulations or real traffic.

Acknowledgements

This work has received funding from the KAUST Office of Sponsored Research under Award No. OSR-2019-CRG8-4033, VINNOVA within the FFI program under contract 2014-06200, the Swedish Research Council, the Swedish Foundation for Strategic Research, Knut and Alice Wallenberg Foundation, and the European Research Council (ERC) under the European Union's Horizon 2020 research and innovation programme (grant agreement 694209), http://scalefreeback.eu.

References

[1] A. Talebpour and H. S. Mahmassani, "Influence of connected and autonomous vehicles on traffic flow stability and throughput," *Transportation Research Part C: Emerging Technologies*, vol. 71, pp. 143–163, 2016.

[2] M. Berrazouane, K. Tong, S. Solmaz, M. Kiers, and J. Erhart, "Analysis and initial observations on varying penetration rates of automated vehicles in mixed traffic flow utilizing sumo," in *2019 IEEE International Conference on Connected Vehicles and Expo (ICCVE)*. IEEE, 2019, pp. 1–7.

[3] P. A. Lopez, M. Behrisch, L. Bieker-Walz, J. Erdmann, Y.-P. Flötteröd, R. Hilbrich, L. Lücken, J. Rummel, P. Wagner, and E. Wießner, "Microscopic traffic simulation using sumo," in *2018 21st International Conference on Intelligent Transportation Systems (ITSC)*. IEEE, 2018, pp. 2575–2582.

[4] M. J. Lighthill and G. B. Whitham, "On kinematic waves II. a theory of traffic flow on long crowded roads," *Proceedings of the Royal Society of London. Series A. Mathematical and Physical Sciences*, vol. 229, no. 1178, pp. 317–345, 1955.

[5] D. Helbing, A. Hennecke, V. Shvetsov, and M. Treiber, "Micro-and macro-simulation of freeway traffic," *Mathematical and computer modelling*, vol. 35, no. 5-6, pp. 517–547, 2002.

[6] R. M. Colombo and E. Rossi, "On the micro-macro limit in traffic flow," *Rendiconti del Seminario Matematico della Università di Padova*, vol. 131, pp. 217–235, 2014.

[7] S. Fan, M. Herty, and B. Seibold, "Comparative model accuracy of a data-fitted generalized aw-rascle-zhang model," *Networks and Heterogeneous Media*, vol. 9, no. 2, pp. 239–268, 2014.

[8] J.-P. Lebacque, J. Lesort, and F. Giorgi, "Introducing buses into first-order macroscopic traffic flow models," *Transportation Research Record: Journal of the Transportation Research Board*, no. 1644, pp. 70–79, 1998.

[9] M. L. Delle Monache and P. Goatin, "Scalar conservation laws with moving constraints arising in traffic flow modeling: an existence result," *Journal of Differential equations*, vol. 257, no. 11, pp. 4015–4029, 2014.

[10] G. Piacentini, P. Goatin, and A. Ferrara, "Traffic control via moving bottleneck of coordinated vehicles," in *15th IFAC symposium on control in transportation systems*, 2018.

[11] M. Čičić and K. H. Johansson, "Traffic regulation via individually controlled automated vehicles: a cell transmission model approach," in *21st International Conference on Intelligent Transportation Systems (ITSC)*, Maui, US, 2018.

[12] M. Garavello, P. Goatin, T. Liard, and B. Piccoli, "A multiscale model for traffic regulation via autonomous vehicles," *Journal of Differential Equations*, vol. 269, no. 7, pp. 6088–6124, 2020.

[13] V. L. Knoop and W. Daamen, "Automatic fitting procedure for the fundamental diagram," *Transportmetrica B: Transport Dynamics*, vol. 5, no. 2, pp. 129–144, 2017.

[14] T. Seo, Y. Kawasaki, T. Kusakabe, and Y. Asakura, "Fundamental diagram estimation by using trajectories of probe vehicles," *Transportation Research Part B: Methodological*, vol. 122, pp. 40–56, 2019.

[15] K. Fadhloun, H. Rakha, and A. Loulizi, "Macroscopic analysis of moving bottlenecks," *Transportation letters*, vol. 11, no. 9, pp. 516–526, 2019.

[16] M. Čičić and K. H. Johansson, "Front-tracking transition system model for traffic state reconstruction, model learning, and control with application to stop-and-go wave dissipation," *Transportation Research Part B: Methodological*, 2021, submitted.

[17] H. Holden and N. H. Risebro, *Front Tracking for Hyperbolic Conservation Laws*. Springer, 2015, vol. 152.

[18] M. Treiber, A. Hennecke, and D. Helbing, "Congested traffic states in empirical observations and microscopic simulations," *Physical review E*, vol. 62, no. 2, p. 1805, 2000.